Evaluation of Control Methods for Isolated Three-phase AC-DC converter using Modular Multilevel Converter Topology

Toshiki Nakanishi
Dept. of Electrical, Electronics and Information Engineering
Nagaoka University of Technology
Nagaoka Niigata, Japan
nakanishi@stn.nagoakaut.ac.jp

Jun-ichi Itoh
Dept. of Electrical, Electronics and Information Engineering
Nagaoka University of Technology
Nagaoka Niigata, Japan
itoh@vos.nagaokaut.ac.jp

Abstract— **This paper discusses a novel isolated three-phase AC-DC converter using Modular Multi-level Converter (MMC) topology for a medium voltage application. The MMC at a primary stage of an isolated AC-DC converter can directly convert a three-phase AC into a high-frequency AC voltage of 1 kHz. In this paper, the features of the proposed circuit are discussed according to the voltage ratings of the switching devices. Moreover, the total harmonic distortion (THD) of the input current, the output voltage, the number of cells and the capacitance of the DC capacitor are evaluated on each switching devices in the proposed system. Finally, the proposed system performance with SiC MOSFET of 3.3 kV is demonstrated by the simulation. As a result, the proposed converter achieves the low THD of the input current waveform which is approximately 2.64%.**

Kywords—Modular Multi-level converter; Capacitor Voltage Control; Direct Power Conversion; H-bridge Cell; Isolated Three-phase AC-DC converter;

I. INTRODUCTION

Recently, the multi-level converter topologies have been discussed actively in the medium voltage application such as 3.3 kV or 6.6 kV [1-4]. However, the conventional high power converters have some disadvantages: (i) the malfunctions or failures of other power conversion due to harmonics disturbance, and (ii) the cost is high due to high voltage rating devices and passive components. On the other hand, the multi-level converters are able to decrease the harmonic distortions and volumes of the input or output filters. Moreover, the voltage stress of a switching device can be reduced. Therefore, switching devices, which are high speed switching and the low rated voltage can be used in the multi-level converters. However, the circuit configuration of the multi-level converter becomes complicated because the number of the circuit components increase proportional to the power capacity. Thus, it is difficult to increase the power capacity for the conventional multi-level converter topologies.

In order to solve this problem, Modular Multi-level Converter (MMC) has been proposed as one of the multi-level converter topologies [5]. The advantages of the MMC are follows; (i) the circuit configuration is simpler than other multi-level converters because of the cascade connection of each cell which is constructed from switching devices and a DC capacitor. (ii) The MMC can reduce the harmonic distortions in the output voltage due to use of many voltage levels which is similarly to the multi-level converters. Therefore, the MMC topology can be applied in high capacity power applications; such as Static synchronous Compensator (STATCOM) and medium adjustable speed drive systems [6-9].

However, the high power converters which use MMC result that the volume of the converters becomes larger due to the huge transformer which is operated with line-frequency between the grid and the converter for safety purpose. In order to reduce the size of the transformer, a high frequency operation of converter is effective. Furthermore, a small and simple transformer can be used by applying a high frequency link of single-phase. However, three-phase to single-phase AC-AC direct power converters using MMC which convert commercial frequency AC voltage into high frequency voltage have not been so many reported [10].

This paper proposes a novel isolated three-phase AC-DC converter using MMC and the control strategy. Three-phase to single-phase MMC topology is used at primary stage in the isolated AC-DC converter. The proposed system can directly convert an input three-phase voltage into a high frequency single-phase voltage of 2.6 kV and 1 kHz. Furthermore, the volume of the proposed system can become small due to high frequency transformer. In addition, the input current and the DC capacitor voltage of the cells can be controlled independently. This paper organized as follows; first, the circuit topology of the MMC is explained. Second, each of the control strategy which controls the input current, the cell capacitor voltage and the output voltage of the MMC, are described. Finally, the comparative evaluations of the system design based on the rated voltage of switching devices are considered. In particular, the numbers of cells and switching devices, the electrostatic energy of the DC capacitors, the THD of the input current and the efficiency considering the loss at switching devices are evaluated when high rated voltage devices: 2.5-kV IGBT, 3.3-kV IGBT and 3.3-kV SiC-MOSFET are applied to the proposed system.

978-1-4799-0482-2/13/$31.00 ©2013 IEEE

II. MAIN CIRCUIT CONFIGURATION

Fig.1(a) shows the circuit configuration of the isolated three-phase AC-DC converter using MMC topology. E Each leg consists of two interconnection reactors L_b and H-bridge cells. Then, each of the leg is connected to a load in parallel. Due to the cascade connection of cells, the proposed converter can achieve a multi-level voltage waveform and also can reduce the rated voltage of each cell. Thus, increasing the numbers of the cascaded cells are benefits because the harmonic distortions can be reduced, and low voltage rating switching devices can be applied.

Furthermore, the proposed system can directly convert an input three-phase voltage into a high frequency single-phase voltage. Therefore, a high frequency transformer can be applied. Moreover, the volume of the proposed system can become small due to the high frequency transformer. In addition, it is able to be isolated between an input side and an output side by the high frequency transformer.

The proposed system can control each arm group separately. In this paper, the arm group on the upper side is defined a group A, the arm group on the downside is defined a group B.

Fig.1(b) shows a configuration of the H-bridge cell. Each cell consists of four switching devices and a DC capacitor. The output voltage of each cell is controlled by pulse width modulation (PWM). Furthermore, it is necessary to keep the capacitor voltage constantly in order to operate the main circuit.

III. CONTROL STRATEGY

Fig. 3 shows the control block of the proposed converter. The proposed control is applied to each arm group A and B as shown in Fig. 1. The proposed control block diagram is separated into two blocks, the capacitor voltage control block and the input current control block. Moreover, the capacitor voltage control block uses two controls, namely an average control and a balance control [5].

A. Average Voltage Control

The average voltage control corrects the error between the average value of the capacitors voltage in each arm group and the voltage command that is generated from a PI control. The average value of the capacitors voltage v_{c_ave} is given by (1).

$$v_{c\_ave} = \frac{1}{3}\sum_{m=1}^{n/2}\left(v_{crm} + v_{csm} + v_{ctm}\right) \tag{1}$$

where n is the number of cells at each leg and v_{crm}, v_{csm} and v_{csm} are each capacitor voltage in the each arm. The number of cells is set $n/2$ to calculate the average value of the capacitors voltage in each arm group because each arm group is independently controlled.

B. Balance Voltage Control

The average voltage control is used to keep the voltage of all capacitor voltage. However, an unbalance voltage which occurs among the capacitors cannot be suppressed by the average voltage control only because the average control corrects only the error between the average value of the capacitors voltage in each group in subjects to the voltage command. Therefore, the balance voltage control is used to correct the error between each of the capacitors voltage and the voltage command.

$$v_{ce\_km} = K_C\left(v_c^{*} - v_{c\_km}\right) i_k \quad \mathrm{k = r,s,t} \quad m = 1,2,\ldots n/2 \tag{2}$$

where v_{crm}, v_{csm} and v_{csm} are each capacitor voltage in the each arm, K_C is the gain of the balance voltage control, k is the index of each phase, m is the index of the cell step.

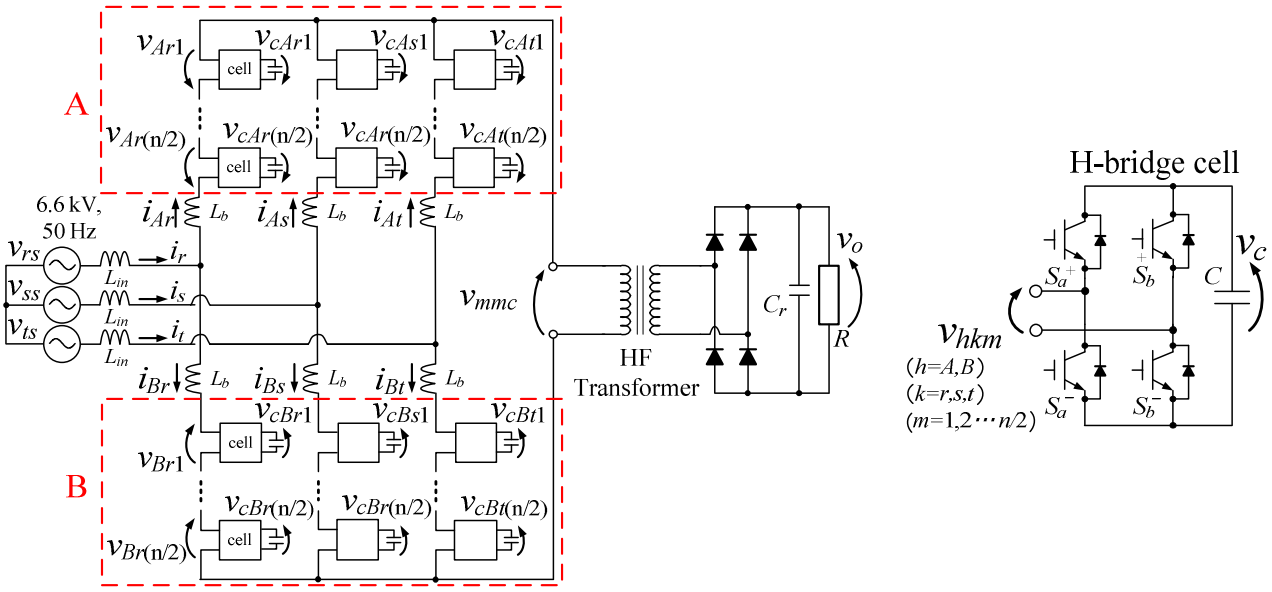

(a) Main circuit configuration. (b) H-bridge cell.

Fig. 1. Circuit diagrams of the proposed circuit for AC-DC isolated converter with MMC topology.

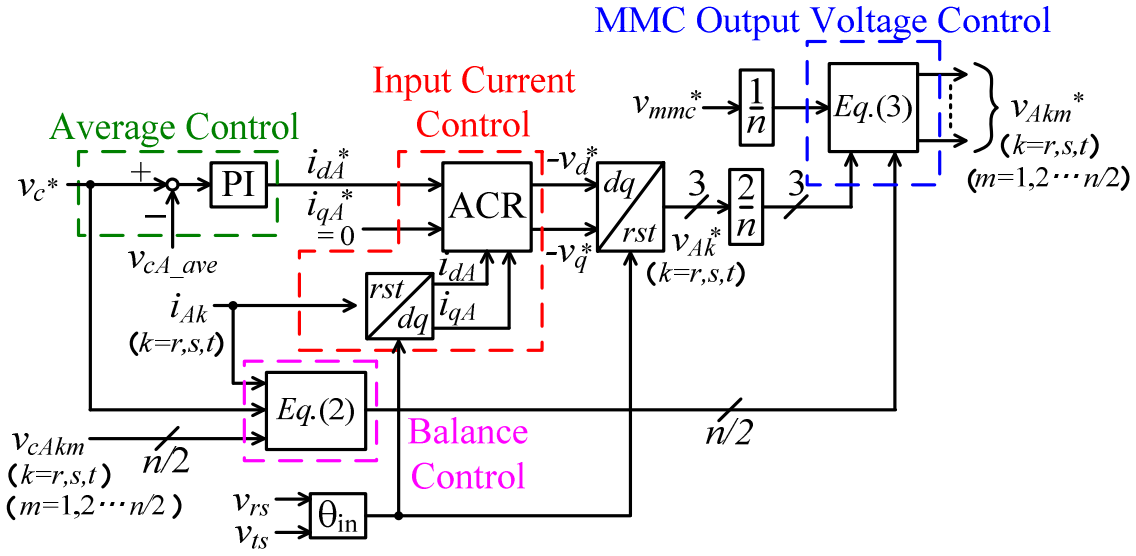

Fig. 2. Control block diagrams of the proposed circuit for the arm group A.

Moreover, the error between the capacitor voltage command v_c^* and each capacitor voltage contains non-linear factor. Therefore, the high response angular frequency has to be set. In the proposed control method, it is possible to achieve the voltage balance by multiply the error by each arm current i_k at the low response angular frequency. Moreover, it is not necessary to erase the error exactly because the balance control is the auxiliary control for the average voltage control. Therefore, the balance control can be constructed by only a proportional control.

C. Input Current Control

The input current separately flows to the upper side arm and the downside arm in each phase. Therefore, the input current can be determined by controlling the current which flow in buffer reactors. In addition, the input current control does not need the link operation between the group A and the group B. Furthermore, the control systems are able to separate between the group A and the group B.

The input current control is implemented by PI controllers, and the compensators for the cross terms of i_d and i_q which are provided from the transformation of rotating frame. The input current control is separated into the active current control (i_d) and the reactive current control (i_q). The reactive current i_q^* is set to zero to control the input power factor to 1 and to reduce the absolute value of the input current.

Therefore, the same input current command is given to each cell because cascaded cells control the common arm current.

D. MMC Output Voltage Control

The same command of the MMC output voltage control is given to each cell in order to convert a three-phase input voltage to a high frequency voltage. The output voltage of a cell is required v_{mmc}^*/n when the command of the MMC output voltage control is v_{mmc}^* and the number of cells in a leg is.

Finally, the output voltage of the cell is given by (3). Note that the sign of the MMC output voltage command v_{mmc}^* has to be changed because the direction of cell output voltage is different in the group A and the group B.

$$\begin{aligned} v_{Akm} &= \frac{1}{n}\left(2v_{Ak} + v_{mmc}^* - v_{ce\_Akm}\right) \\ v_{Bkm} &= \frac{1}{n}\left(2v_{Bk} - v_{mmc}^* - v_{ce\_Bkm}\right) \end{aligned} \qquad k = r,s,t \quad m = 1,2,\ldots n/2 \quad (3)$$

E. Capacitor Voltage Command

The MMC output voltage command v_{mmc}^* that uses to obtain the high frequency output voltage is added to the output block of the input current control. The change of voltage value in each cell depends on the number of cells at each leg since the cells are connected to the load in series. In addition, each capacitor voltage also depends on the input and output voltage. The capacitor voltage command v_c^* is given by (4).

$$v_c^* \geq \frac{1}{n}\left(2\sqrt{\frac{2}{3}}E + V_{mmc}\right) \quad (4)$$

where E is an effective value of the input line to line voltage, V_{mmc} is a maximum value of the MMC output voltage command and n is the number of cells at each leg. From (4), the output voltage of each cell becomes smaller as the numbers of cells increase. Therefore, the capacitor voltage command can be lower.

IV. Evaluation of the Proposed System

A. Evaluation Condition

In the proposed system, from (4), the capacitor voltage is depends on the input current control and the MMC output voltage control. Therefore, the rated voltage of the switching

device is depends on the capacitor voltage of the cell. In cases where the high rated voltage devices are applied, it is possible to reduce the number of the circuit components in the proposed system. On other hand, in cases where the low rated voltage devices are applied and the number of cells increases, it is possible to suppress the harmonic distortion of the input current due to the high speed switching and many voltage levels with using the low voltage rating devices. Thus, the design factors: the number of cells, the capacitor voltage and the THD of the input current are different. Therefore, the comparing of the circuit performance based on the rated voltage of switching devices is required. In comparison of the circuit performance, some IGBTs with the high rated voltage and SiC with the rated voltage 3.3 kV are employed.

The conditions in order to compare the circuit performance are as follow.

a) The rated voltages of IGBT are 2.5 kV, 3.3 kV and 6.5 kV.

b) The capacitor voltage is set 20% more than the value which is calculated by (4). Moreover, the rated voltage is set 30% more than the capacitor voltage.

c) The ripple of the capacitor voltage is within 2% against the average value of the capacitor voltage.

d) The output power is set 400 kW and the output voltage is set 450 V.

e) MMC output voltage command v_{mmc}^{*} is set 2.6 kV, 1 kHz.

f) Buffer reactor L_b is 1 mH (the percent impeadance $\%Z = 0.62$ in all system.).

g) Each cell has only one DC capacitor.

B. Comparative Evaluation of the proposed system

The numbers of cells, switching devices and DC capacitors are found by (4) and condition b).

Table 4 shows the comparison result for the number of cells and switching devices depending on the rated voltage of the switching device.

In cases where IGBTs with the rated voltage of 2.5 kV are applied, 10 cells are required per leg. Moreover, 120 IGBTs are required. On other hand, 2.5-kV IGBT is able to be set the high response angular frequency due to a high speed switching. Therefore, it is possible to reduce the value of buffer reactors and DC capacitors.

On other hand, in cases where IGBTs with the rated voltage of 3.3 kV are applied, 8 cells per leg and 96 IGBTs are required. The number of cells and switching devices can be reduced compared with that of 2.5-kV IGBT. However, the switching frequency is limited because the switching speed is lower than that of 2.5-kV IGBT. Therefore, it is necessary to increase the value of DC capacitors since the response angular frequency of the control system is low.

In cases where IGBTs with the rated voltage of 6.5 kV are applied, 4 cells per leg and 48 IGBTs are required. The number of cells and switching devices can be significantly reduced compared with that of 2.5-kV IGBT and 3.3-kV IGBT.

Table 1. Device Parameters and switching frequency.

	Device Parameters	f_s
2.5-kV IGBT CM400DY-50H	V_{CE}=2.5kV, I_c=400A, E_{on} = 500 mJ @ Ic = 400 A, V_{CE} = 1.25kV, R_{Gon} = 7.5 Ω, V_{GE} = ±15 V E_{off} = 400 mJ @ Ic = 400 A, V_{CE} = 1.25kV, R_{Goff} = 7.5 Ω, V_{GE} = ±15 V	9 kHz
3.3-kV IGBT CM800E2C-66H	V_{CE}=3.3kV, I_c=800A, E_{on} = 1200 mJ @ Ic = 800 A, V_{CE} = 1.65kV, R_{Gon} = 2.5Ω, V_{GE} = ±15 V E_{off} = 1000mJ @ Ic = 800 A, V_{CE} = 1.65kV, R_{Goff} = 2.5 Ω, V_{GE} = ±15 V	3 kHz
6.5-kV IGBT FZ400R65KE3	V_{CE}=6.5kV, I_c=400 A, E_{on} = 3450 mJ @ Ic = 400 A, V_{CE} = 3.6kV, R_{Gon} = 1.9 Ω, V_{GE} = ±15 V E_{off} = 2250 mJ @ Ic = 400 A, V_{CE} = 3.6kV, R_{Goff} = 13 Ω, V_{GE} = ±15 V	1 kHz

Table 2. Comparison for numbers of cells and switching devices depending on the rated voltage of the switching device.

Rated Voltage	Numbers of Cells @leg	Numbers of Switching devices
2.5 kV	10	120
3.3 kV	8	96
6.5 kV	4	48

However, the switching speed of 6.5-kV IGBT is lower than 2.5-kV IGBT and 3.3-kV IGBT. Furthermore, the large value of DC capacitor has to be applied since the response angular frequency of the average control ω_{AVR} becomes low. In addition, the large inductance of buffer reactors are also applied since the response angular frequency of the input current control ω_{ACR} becomes low. In proposed system, MMC outputs a high frequency voltage. However, the voltage drop becomes large since a voltage-dividing occur between the high frequency transformer and buffer reactors. In the worst case, it is difficult to transmit a high frequency power to secondary side of transformer when buffer reactors are large. Therefore, it is necessary to reduce the inductance of buffer reactors to transmit the high frequency power.

To conclude, high rated voltage devices with a low switching speed are unfitted for the proposed circuit.

C. Evaluation of the proposed system by appling SiC devices

SiC devices have some advantages: the high rated voltage, the low loss, the high switching speed. Therefore, many applications of SiC devices are considered. Especially, it is expected to apply SiC devices to a high voltage and high power conversion system depending on the high device performance. Recently, SiC-MOSFET with the rated voltage of 10 kV has been developed [11]. However, *dv*/*dt* at winding wires of the high frequency transformer becomes greatly large and the insulation degradation among winding wires may occur when the proposed system is operated by the high rated voltage devices. From considering of the previous chapter, it is desirable to set the switching frequency of 9 kHz to operate the high frequency transformer in 1 kHz. Therefore, it is necessary to consider the operation of the proposed system in the case of applying 3.3-kV SiC-MOSFET [12] to the proposed system.

Fig. 3 shows the comparison result of total energy which all capacitor charges. The total electrostatic energy E_C is given by (5)

$$E_c = \frac{1}{2} C V_c^2 \times N \tag{5}$$

where C is a capacitance of each capacitor, N is the number of capacitors in MMC and V_C is the average value of the capacitor voltage. V_C is equal to the capacitor voltage command v_c^* when all capacitor voltage is kept constant by the average control and the balance control.

From the comparison result, the total electrostatic energy is the largest when 3.3-kV IGBTs are applied. In the case of applying 3.3-kV IGBTs, the large capacitance has to be set since the response angular frequency of the average control ω_{AVR} becomes low.

In the case of applying 2.5-kV IGBTs to the proposed system, the total electrostatic energy is lower than that of 3.3-kV IGBTs since the capacitance C and the capacitor voltage V_C become lower than that of 3.3-kV IGBTs. However, the ripple voltage against the average value of the capacitor voltage becomes large. Therefore, the capacitance cannot be reduced greatly compared with that of 3.3-kV IGBTs.

In the case of applying 3.3-kV SiC-MOSFETs to the proposed system, the total electrostatic energy is the lowest since the number of cells and the ripple voltage against the average value of the capacitor voltage can be reduced. Furthermore, applying the 3.3-kV SiC-MOSFETs to the system can achieve the downsizing of the proposed system since the number of circuit components can be reduced and the heat loss at switching devices is suppressed.

V. Opreration Evaluation by Simulation

A. Fundamental Operation

Table 3 shows the simulation parameters. The switching frequency of SiC-MOSFET is set to 9 kHz. Note that the ideal elements are used in the switching device. In addition, the output voltage command is a square-wave of 2.6 kV, 1 kHz.

Fig. 4 shows the input phase voltage and current waveforms. From Fig. 5, it is confirmed that the unity power factor can be obtained in the input stage. Moreover, the total harmonic distortion (THD) of the input current is approximately 2.64 %. The input current waveform includes a few of pulse-beat. However, the pulse-beat does not affect the THD of the input current since the frequency of the pulse-beat is very high order compared with the fundamental frequency.

Fig. 5 shows the output voltage waveform. From the result, the output voltage is constantly controlled at approximately 450 V. Thus, the power conversion from three-phase AC waveforms into a DC waveform can be confirmed.

Fig. 6 shows the voltage waveforms of the cell capacitor which are connected to the r-phase. The cell capacitor voltages are controlled accordingly to the capacitor voltage command v_c^* by the average control and the balance control. In the capacitor voltage, the ripples include two frequency components: 100 Hz and 1 kHz. Then, the ripple of 1 kHz is smaller than that of 100 Hz. Furthermore, the ripple of 100 Hz comprises a majority of the capacitor voltage ripple. However, the maximum ripple of each capacitor voltage is obtained by 2.0 %. Thus, it is confirmed that the voltage ripple does not affect the circuit operation in the proposed system.

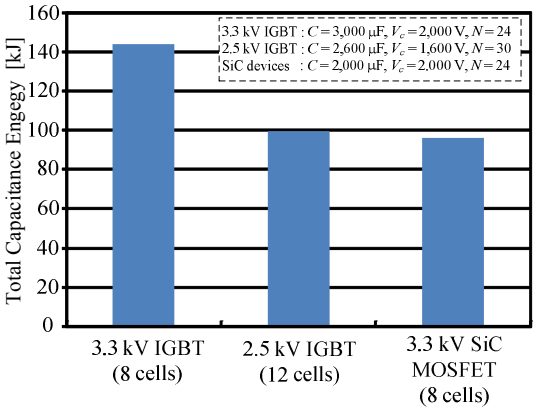

Fig. 3. Comparison of total electrostatic energy in DC capacitors according to the switching device.

Table 3 Simulation parameters

Output power	400 kW	Input voltage rms	6.6 kV
Input voltage frequency	50 Hz	Output voltage	450 V
Number of cell per leg n	8	DC capacitor C	2 mF
Load R	0.5 Ω	Output capacitor C_r	3 mF
Turn ration pri.: sec.	3.6 : 1	Carrier frequency	9 kHz
Interconnection reactor L_{in}			4.5 mH (%Z = 1.38)
Buffer reactor L_b			1 mH (%Z = 0.62)
Leakage inductance at primary of the transformer			36 μH
Leakage inductance at primary of the transformer			10 μH

Fig. 7 shows the output voltage waveforms of MMC, it can be confirmed that the high frequency AC voltage which is 1 kHz is obtained. However, the error between the output voltage of the MMC and the command occur. This is the reason that the voltage drops in each buffer reactor. Moreover, the output voltage waveform is dropped when the voltage polarity changes. This is the reason that the high frequency current flows in all diode of the rectifier circuit due to the action of the leakage inductance of the high frequency transformer. The voltage is depended on the voltage drop of the leakage inductance.

B. Comparison with respect to THD of Input Current

Fig. 8 shows the comparison result with respect to THD of the input current. From Fig. 8, The THD is the lowest in cases where IGBTs with the rated voltage of 2.5 kV. In the system which is applied of 2.5-kV IGBTs, the number of cells is the highest. Furthermore, the harmonic distortion is suppressed since the input voltage becomes multi-level waveform due to multi-cells. On the other hand, the system which is applied SiC-MOSFETs can improve the THD of the input current compared with the system which is applied 3.3-kV IGBTs since it is possible to set the response angular frequency the

input current control ω_{ACR} to high due to the high switching speed.

C. Comparison Evaluation of Efficiency

Fig. 9 shows the Efficiency comparison of the proposed system considering the loss at switching devices.

Fig. 10 shows comparison result of the switching loss and the conduction loss.

In the case of applying 2.5-kV IGBTs to the proposed system, the loss at which occur at the switching device is the larger than other one. This is because the system which is applied 2.5-kV IGBTs has the largest number of switching device and the switching frequency is high. Therefore, the efficiency of the system which is applied 2.5-kV IGBTs is the lower than other one.

In the case of applying 3.3-kV IGBTs to the proposed system, the loss at switching devices is smaller than the system which is applied 2.5-kV IGBTs. From the table 1, both the turn-on loss and the turn-off loss are larger than that of 2.5 kV-IGBTs. However, the total loss of 3.3 kV IGBTs is lower than the total loss of 2.5-kV IGBTs because the switching frequency is lower than that of 2.5-kV IGBTs. Therefore, it is expected for the system which is applied 3.3 kV IGBTs to achieve the high efficiency of 92.9%.

In the case of applying 3.3-kV SiC-MOSFETs to the proposed system, the loss at switching devices is the lowest because both the turn-on loss and the turn-off loss are lower than the loss of both IGBTs. Furthermore, the efficiency is the highest.

In conclusion, applying the 3.3-kV IGBTs or 3.3-kV SiC-MOSFETs is suitable for the proposed system in order to achieve the high efficiency. Moreover, SiC-MOSFET is the most suitable because SiC-MOSFET has the high performance which can reduce the harmonic distortion of the input current, can achieve the high efficiency and the downsizing of the system. On the other hand, 3.3-kV IGBTs also has good performance for the efficiency. Furthermore, it is necessary to consider in more detail in order to achieve reduction of the harmonic distortion of the input current and the downsizing of the system.

V. Conclusion

In this paper, a novel isolated three-phase AC-DC converter using MMC and the control strategy were proposed for a medium voltage application. Three-phase to single-phase MMC topology was used at primary stage in the isolated AC-DC converter. The proposed system could directly convert an input three-phase voltage into a high frequency single-phase voltage. Therefore, the proposed system could reduce the volume of the isolated transformer since the single-phase high frequency transformer could be applied to the high frequency link.

MMC topology was constructed some cells and buffer reactors. The cell was constructed 4 switching devices and DC capacitor. The voltage of the DC capacitor was kept constantly in order to operate MMC. The proposed control system could

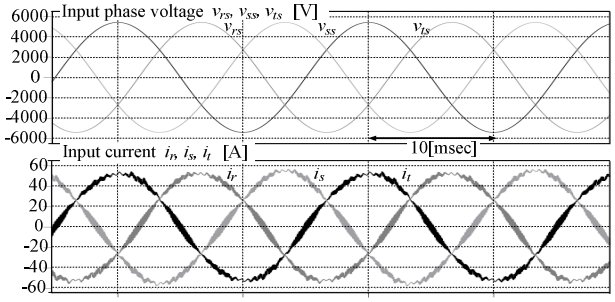

Fig. 4. Waveforms of the input phase voltage and current.

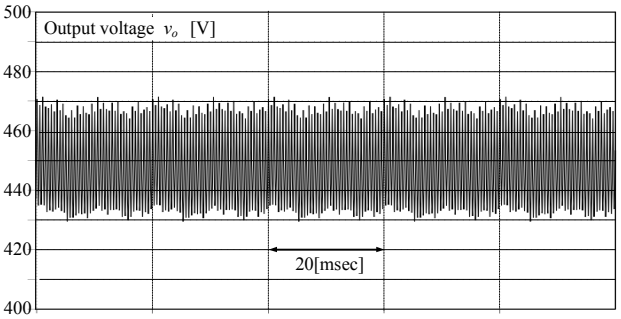

Fig. 5. Waveform of the output voltage at.the diode bridge rectifier

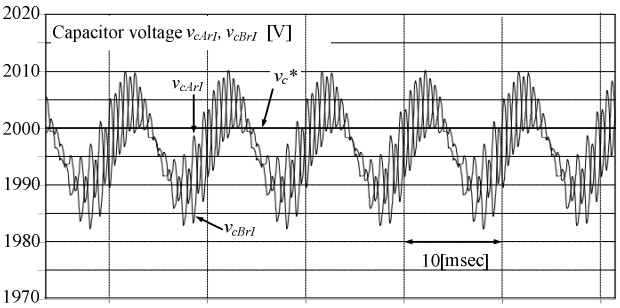

Fig. 6. Waveform of the capacitor voltage.

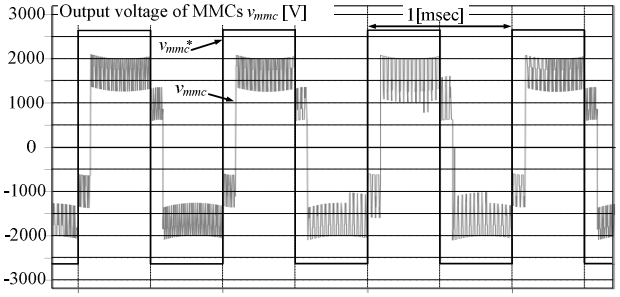

Fig. 7. Waveform of the MMC output voltage.

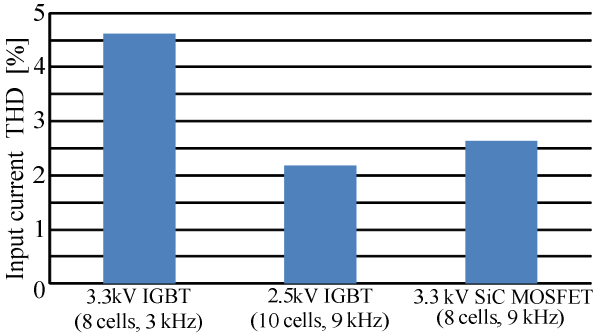

Fig. 8. Comparison of the input current THD according to the switching devices.

control not only the voltage of all DC capacitor but also the input current and the high frequency output voltage of MMC.

The comparison evaluations of the proposed system which is applied each high rated voltage: a 2.5-kV IGBT, a 3.3-kV IGBT and a 3.3-kV SiC-MOSFET were demonstrated by a simulation. As a result, in the case of applying 3.3-kV SiC-MOSFETs to the proposed system, the total electrostatic energy in DC capacitors is the lowest compared with other high rated voltage IGBTs. Furthermore, the system which is applied 3.3-kV SiC-MOSFETs could achieve the downsizing of the proposed system when considering the common value of energy density in all capacitor. Moreover, the system which is applying 3.3-kV SiC-MOSFETs could achieve the low THD input current waveform which is approximately 2.36 % and the maximum ripple factor of each capacitor voltage is approximately 2.0 %. Finally, from Efficiency Comparison result of the proposed system, it was confirmed that the efficiency can be achieved by over 90% by using 3.3 kV IGBTs and 3.3-kV SiC-MOSFET. Furthermore, applying the 3.3-kV IGBTs or 3.3-kV SiC-MOSFETs is suitable for the proposed system in order to achieve the high efficiency. It is necessary for the system which is applying 3.3-kV IGBTs to consider in more detail in order to achieve reduction of the harmonic distortion of the input current and the downsizing of the system.

In future works, the control gain will be optimized. Besides, the effectiveness of the proposed system will be verified by the experimental of the prototype and the optimized design will be considered.

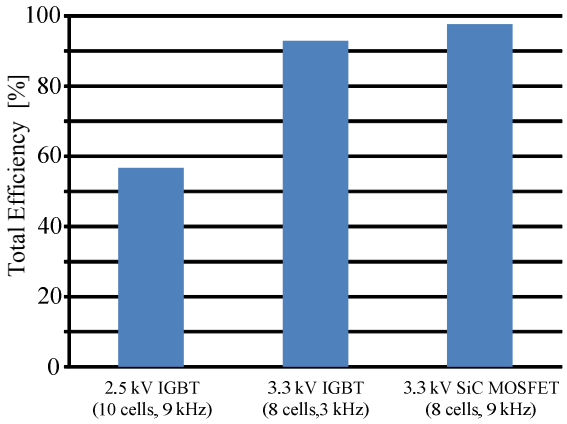

Fig. 9. Efficiency Comparison of the proposed system considering the loss at switching devices.

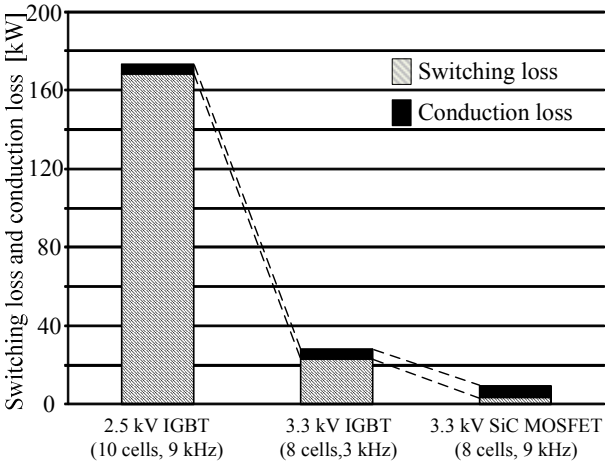

Fig. 10. Comparison of the switching loss and the conduction loss.

REFERECES

[1] P. K. Steimer and M. Winkelnkemper, "Transformerless Multi-Level Converter based Medium Voltage Drives", ECCE2011 pp. 3435 -3441 , (2011)

[2] R.l Crosier, S. Wang and M. Jamshidi, "A 4800-V Grid-Connected Electric Vehicle Charging Station that Provides STACOM-APF Functions with A Bi-directional, Multi-level,Cascaded Converter", APEC2012, pp. 1508-1515R. Nicole, "Title of paper with only first word capitalized," J. Name Stand. Abbrev., in press.

[3] H. M. Pirouz and M. T. Bina, "New Transformerless STATCOM Topology for Compensating Unbalanced Medium-Voltage Loads", Power Electronics and Applications, 2009. EPE '09. 13th European Conference, (2009)

[4] H. Li, Thomas L. Baldwin, C. A. Luongo, and D. Zhang , "A Multilevel Power Conditioning System for Superconductive Magnetic Energy Storage", IEEE Trans. On Applied Superconductivity, Vol. 15, No. 2, pp. 1943-1946 (2005)

[5] M. Glinka and R. Marquardt, "A new ac/ac multilevel converter family", IEEE Trans. Industrial Electronics, vol. 52, No. 3, pp. 662–669, (2005)

[6] M. Hagiwara and H. Akagi, "Control and Experiment of Pulsewidth-Modulated Modular Multilevel Converters", IEEE Trans. on Power Electronics, Vol. 24, No. 7, pp. 1737-1746 (2009)

[7] M. Hagiwara, R. Maeda and H. Akagi, "Negative-Sequence Reactive-Power Control by a PWM STATCOM Based on a Modular Multilevel Cascade Converter (MMCC-SDBC)", IEEE Trans. on Industry Applications, Vol. 48, No. 2, pp .720-729 (2012)

[8] Fang Z. Peng, Wei Qian, and Dong Cao, "Recent Advances in Multilevel Converter/Inverter Topologies and Applications", IPEC 2010, pp. 492-501 (2010)

[9] S. Kenzelmann, A. Rufer, M. Vasiladiotis, D. Dujic, F. Canals and Y. R. de Novaes, "A Versatile DC-DC Converter for Energy Collection and Distribution using the Modular Multilevel Converter", Power Electronics and Applications (EPE 2011), Proceedings of the 2011-14th European Conference, (2011)

[10] M. Vasiladiotis, S Kenzelmann, N. Cherix and A. Rufer, "Power and DC Link Voltage Control Considerations for Indirect AC/AC Modular Multilevel Converters", Power Electronics and Applications (EPE 2011), Proceedings of the 2011-14th European Conference, (2011)

[11] M. K. Das, C. Capell, D. E. Grider, R. Raju, M. Schutten, J. Nasadoski, S. Leslie, J. Ostop, A. Hefner ; "10 kV, 120 A SiC Half H-Bridge Power MOSFET Modules Suitable for High Frequency, Medium Voltage Applications", IEEE, ECCE, pp.2689-2692 (2011)

[12] R. Lai, L. Wang, J. Sabate, A, Elasser and L. Stevanovic, "High-Voltage High-Frequency Inverter using 3.3 kV SiC MOSFETs", Power Electronics and Motion Control Conference (EPE/PEMC), 2012, DS2b.6-1 - DS2b.6-5 (2012)